Stress-Strain State of Earth Dams Considering Soil Moisture

Karim Sultanov[1, a)], Sadillakhon Umarkhonov[1, b)]

[1]*Institute of Mechanics and Seismic Stability of Structures named after M.T. Urazbaev, Uzbekistan Academy of Sciences, Tashkent, Uzbekistan*

[a)] Corresponding author: sultanov.karim@mail.ru
[b)] umarkhonov@gmail.com

Abstract. Earth dams are the most commonly constructed type of dam worldwide. They are made from local materials, making them significantly more cost-effective than concrete dams. When designing earth dams situated in seismic zones, it is crucial to pay special attention to their structural integrity. Each earth dam has unique design specifications and location. The Charvak Dam, built in the Tashkent region, plays a vital role in supplying drinking water and electricity to the population. This article focuses on the dynamic analysis of the stress-strain behavior of earth dams under dynamic loads. A developed method for solving wave problems is employed to determine the stress-strain state of earth structures, specifically earth dams. The finite difference method is utilized to create an algorithm for solving problems, along with calculation formulas of the second-order accuracy in time and space. One of the key advantages of this method is its ability to implement complex nonlinear deformation models that account for structural changes and variations in soil moisture content. Using the Charvak Dam as a case study, the distribution of stresses across the dam's cross-section is determined considering its weight. Additionally, the dynamic response of the earth dam under seismic loads is analyzed numerically. The study quantifies the stress-strain state of the dam and tracks the changes in stresses, strains, and displacements at specific points within the dam over time.

INTRODUCTION

The potential for catastrophic consequences resulting from the failure of earth dams places a heightened demand on their reliability, which is reflected in relevant design standards. However, the processes that determine the performance of an earth dam built on natural foundations are still not sufficiently studied. Numerous scientists have conducted research on the strength, deformation and stability of earth dams under the influence of dynamic and static forces [1-15]. Predicting changes in stress and strain within earth dams due to various loads—such as the self-weight of the soil, water pressure, and seismic impacts—relies on understanding the soil's deformability and strength under stress conditions. The distribution of stress and strain is significantly influenced by the physical and mechanical properties of the soil within the dam body and its foundation, as well as by the geometric parameters of the structure, fluctuations in reservoir levels, seismic impacts, and other factors. Numerical methods are employed to assess the stress-strain state of dams. The design justification for the strength of an earth dam must be based on conditions that prevent ultimate limit states. Additionally, stress and strain values should be determined through an analysis of various parameters, including the results of stress-strain state calculations for the earth dam. This article aims to develop a method for analyzing the dynamic behavior of earth dams using the principles of the mechanics of deformable rigid bodies and to provide justification for this approach.

PROBLEM STATEMENT AND SOLUTION

We consider earth dams built on a rigid foundation (see Fig. 1). If the length of the dam is significantly greater than its width and height, its motion can be treated as a plane-strain problem. When seismic forces are applied to the foundations of earth dams (see Fig. 2), the particles within the dam's material begin to move. The equation of motion for an earth dam is as follows:

$$\rho \frac{d\upsilon_x}{dt} = \frac{\partial S_{xx}}{\partial x} + \frac{\partial P}{\partial x} + \frac{\partial \tau_{xy}}{\partial y}, \quad \rho \frac{d\upsilon_y}{dt} = \frac{\partial S_{yy}}{\partial y} + \frac{\partial P}{\partial y} + \frac{\partial \tau_{xy}}{\partial x} - \rho g. \tag{1}$$

Here, υ_x, υ_y are the particle velocities in the x and y directions; S_{xx}, S_{yy}, τ_{xy} are the deviator stress components; ρ is the density of the medium; P is the pressure.

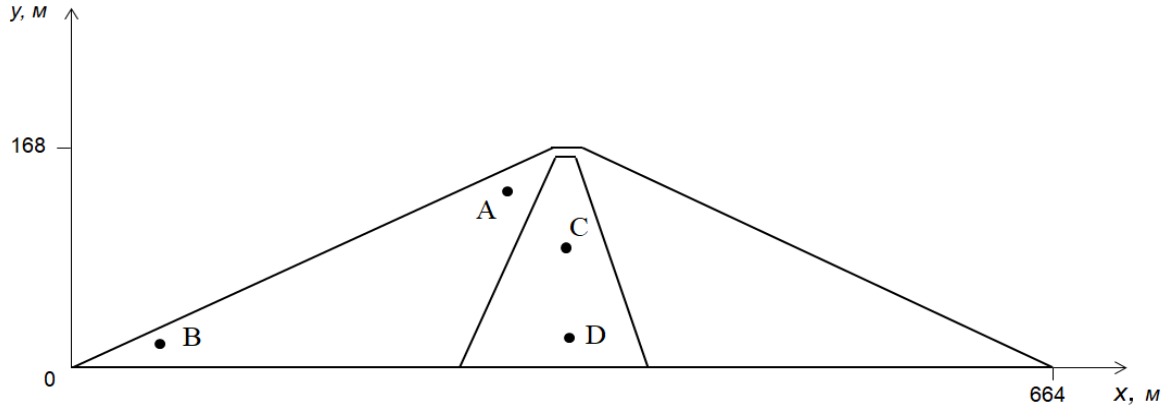

FIGURE 1. Cross-section of an earth dam

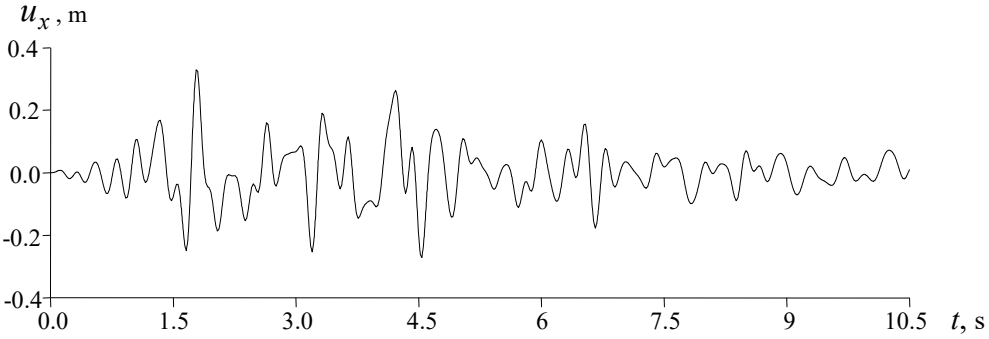

FIGURE 2. Velocigrams recorded during the earthquake at the base of the Charvak Dam

Naturally, the total stresses are determined by the following formulas:

$$\sigma_{xx} = S_{xx} + \mathrm{P}, \quad \sigma_{yy} = S_{yy} + \mathrm{P}, \quad \sigma_{zz} = S_{zz} + \mathrm{P}. \tag{2}$$

The dam deformation model is taken in the form of nonlinear equations:

$$\dot{P} = -\left(\lambda + \frac{2}{3}\mu\right)\frac{\dot{V}}{V}, \tag{3}$$

$$\frac{dS_{xx}}{dt} + \lambda S_{xx} = 2G\left(\frac{d\varepsilon_{xx}}{dt} - \frac{dV}{3Vdt}\right), \quad \frac{dS_{yy}}{dt} + \lambda S_{yy} = 2G\left(\frac{d\varepsilon_{yy}}{dt} - \frac{dV}{3Vdt}\right), \tag{4}$$

$$\frac{dS_{zz}}{dt} + \lambda S_{zz} = 2G\left(\frac{d\varepsilon_{zz}}{dt} - \frac{dV}{3Vdt}\right), \quad \frac{d\tau_{xy}}{dt} + \lambda \tau_{xy} = 2G\frac{d\tau_{xy}}{dt}. \tag{5}$$

The general dependence of the ultimate strength vs pressure in the generalized von Mises condition has the following form:

$$S_{xx}^2 + S_{yy}^2 + S_{zz}^2 + 2\tau_{xy}^2 \le \frac{2}{3}\left[Y(P)\right]^2 \tag{6}$$

$$Y(P) = Y_0 + \frac{\mu P}{1 + \mu P/(Y_{PL} - Y_0)}, \tag{7}$$

Here, K and G are the bulk compression and shear moduli, respectively; $V=\rho_0/\rho$ is the relative volume; Y_0 is the cohesion; μ is the friction coefficient; Y_{PL} is the ultimate shear strength of the rock fill; λ is the functional defined by the following formulas:

$$\lambda = \frac{3W}{2Y^2} H(W), \quad H(W) = \begin{cases} 1, & \text{at } W \geq 0 \\ 0, & \text{at } W < 0 \end{cases}, \quad W = 2\mu \left\{ \sum_{j=x,y,z} S_{jj} \left(\frac{d\varepsilon_{jj}}{dt} - \frac{1}{3} \frac{dV}{Vdt} \right) + \tau_{xy} \frac{d\varepsilon_{xy}}{dt} \right\}. \tag{8}$$

It is necessary to add to the system of equations (1)–(7) the relations linking the components of the strain rates with the mass velocities. The soil continuity equation has the following form:

$$\frac{d\varepsilon_{xx}}{dt} = \frac{\partial U_x}{\partial x}, \quad \frac{d\varepsilon_{yy}}{dt} = \frac{\partial U_y}{\partial y}, \quad \frac{d\varepsilon_{xy}}{dt} = \frac{1}{2}\left(\frac{\partial U_y}{\partial x} + \frac{\partial U_x}{\partial y} \right). \tag{9}$$

$$\cdot \frac{dV}{dt} - V \cdot \left(\frac{\partial U_x}{\partial x} + \frac{\partial U_y}{\partial y} \right) = 0 \ . \tag{10}$$

Consider the mechanical parameters of soil as functions depending on the moisture content in the following form:

$$K(I_W) = K_{sat} \exp(\alpha_K (1 - I_W)) \tag{11}$$

$$G(I_W) = G_{sat} \exp(\alpha_G (1 - I_W)) \tag{12}$$

$$c(I_W) = c_{sat} \exp(\beta(1 - I_W)) \tag{13}$$

$$\mu(I_W) = \mu_{sat} \exp(\gamma(1 - I_W)) \qquad I_W = W/W_{sat} \tag{14}$$

$$Y(P, I_W) = c(I_W) + \mu(I_W) \cdot P \tag{15}$$

Here, K_{sat} is the modulus of volume compression, G_{sat} is the modulus of shear, c_{sat} is the cohesion force, μ_{sat}- is the coefficient of the angle of internal friction of completely saturated soil. I_W is the parameter of the extent of soil moisture content; W is the current soil moisture content; W_{sat} is the moisture content corresponding to complete water saturation.

Thus, the system of differential equations (1)–(15) is closed and, with initial and boundary conditions, describes the pattern of dynamic behavior and stress-strain state of an earth dam. The slopes and crest of the dam are assumed to be stress-free. The initial conditions are assumed to be zero.

The geometric dimensions of the earth dam are: height – 168 m, upper section width – 12 m, lower section width – 664 m, upper slope – 1:2, lower slope – 1:1.9, central core widths – 110 and 12 m. The following physical and mechanical parameters of the earth dam were taken: for the slope: the density - 1980 kg/m^3, the modulus of elasticity -E_{dam}=6210 MPa, the Poisson's ratio - ν_{dam}=0.3. The slope strength indicators (cohesion, friction coefficient, ultimate shear strength) were $Y0=\mu/800$, μ=0.4, $Y_{dam}=20Y_0$. For the core: the density - 1760 kg/m^3; the modulus of elasticity - E_{core}=3105 MPa; the Poisson's ratio - ν_{core}=0.3. The slope strength indicators (cohesion, friction coefficient, ultimate shear strength) were $Y_0=\mu/1000$, μ=0.3, $Y_{core}=20Y_0$.

RESULTS

We will consider numerical solutions to the dynamic problems posed, using the finite difference method and the scheme proposed by M. Wilkins for a quadrilateral mesh. In non-stationary problems, one independent variable—time (*t)* - is particularly important. Discretization of the problem with respect to this variable means that the calculation is performed with discrete time steps, each representing the transition from the state at time t_0 to the state at time $t_0 + \Delta t$. The advantage of Wilkins' scheme is that the time step Δt is automatically determined during the calculation process based on stability and accuracy, allowing it to be adjusted as needed.

To solve the static problem, we used the Plaxis 2D program, which is based on the finite element method. In this case, the water pressure and moisture content of the earth dam were taken into account.

For the dynamic forces, we applied harmonic forces. When a harmonic load is applied to the foundation of an earth dam, it causes movement in the particles within the dam body, resulting in deformation of the soil inside the dam.

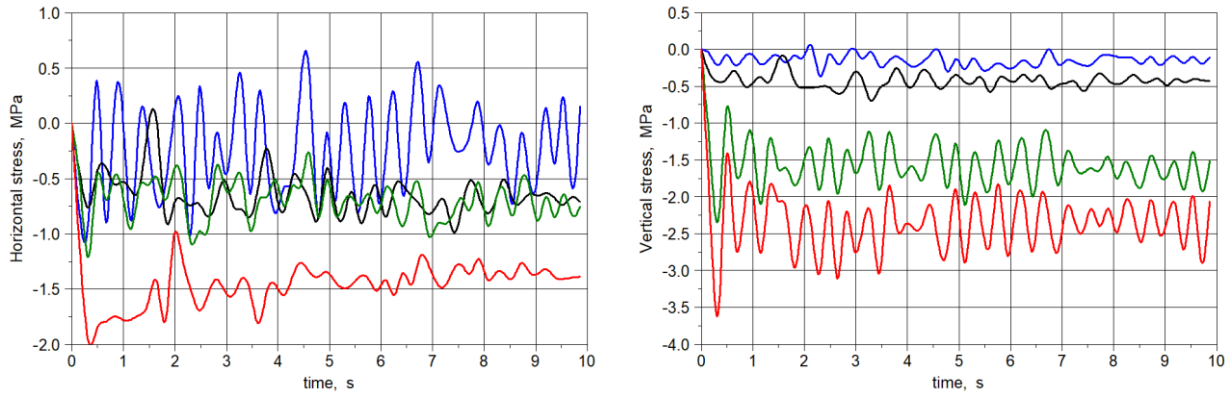

(a) (b)

FIGURE 3. Change in horizontal (a) and vertical (b) stresses over time.
The blue line is point A, the green line is point B, the black line is point C, and the red line is point D.

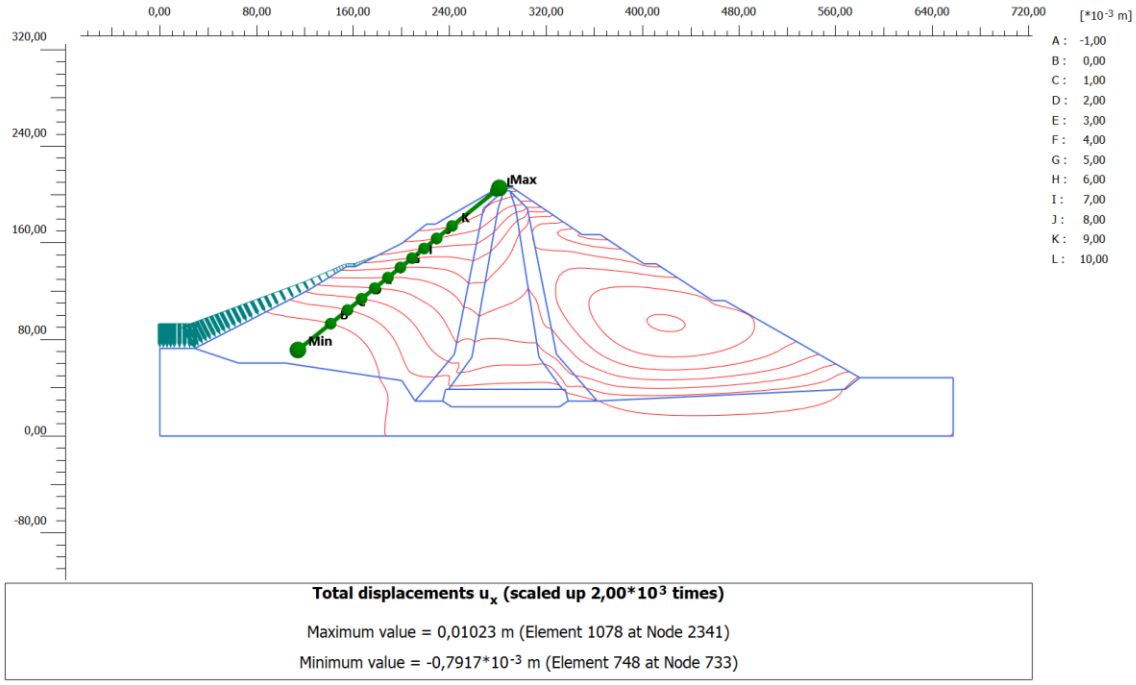

FIGURE 4. Isolines of horizontal displacements on the cross-section of the dam

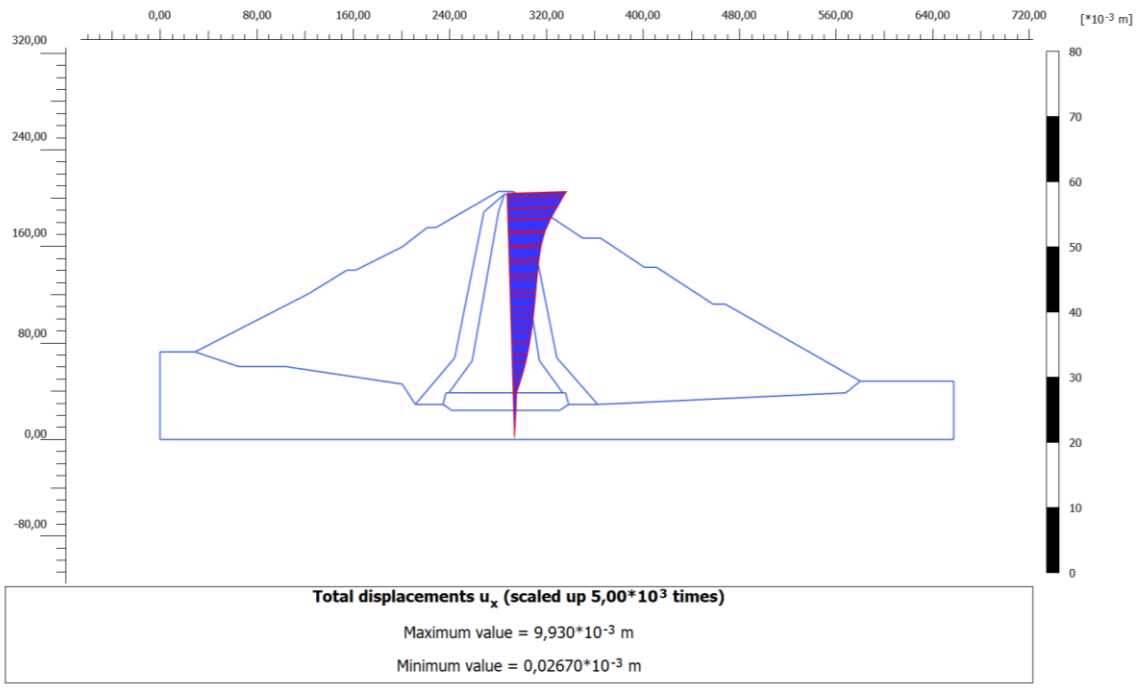

FIGURE 5. Horizontal displacement diagram in the middle of an earth dam

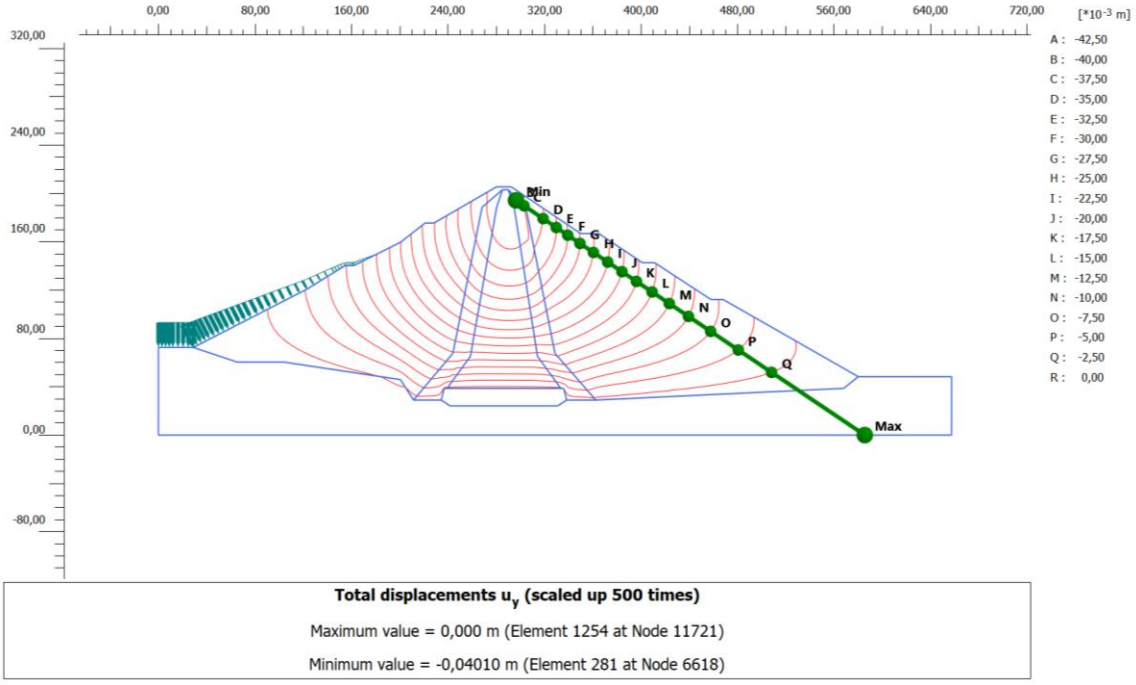

FIGURE 6. Isolines of vertical displacements of an earth dam on the cross-section of the dam

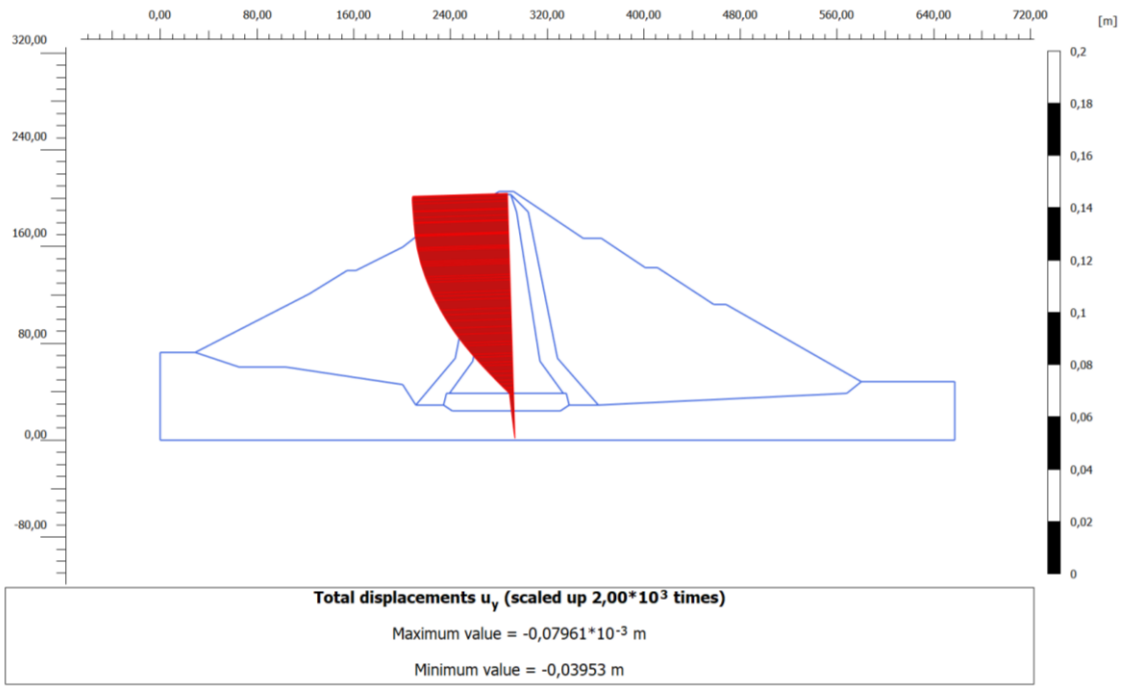

FIGURE 7. Vertical displacement diagram at the middle of an earth dam

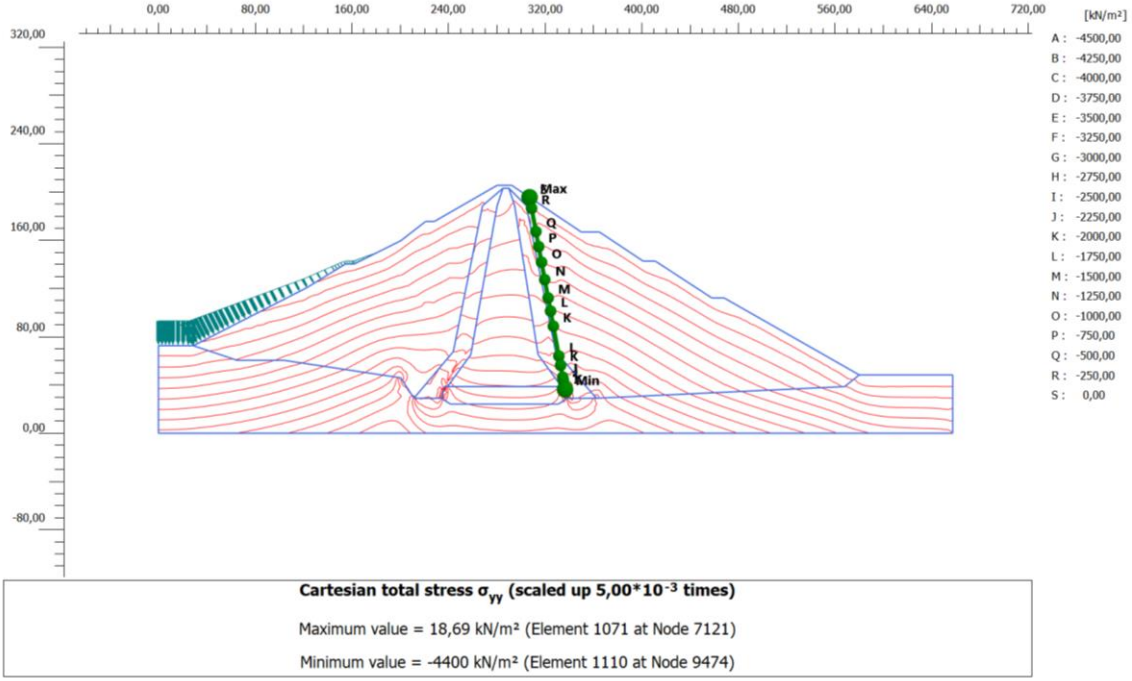

FIGURE 8. Isolines of vertical stresses of an earth dam on the cross-section of the dam

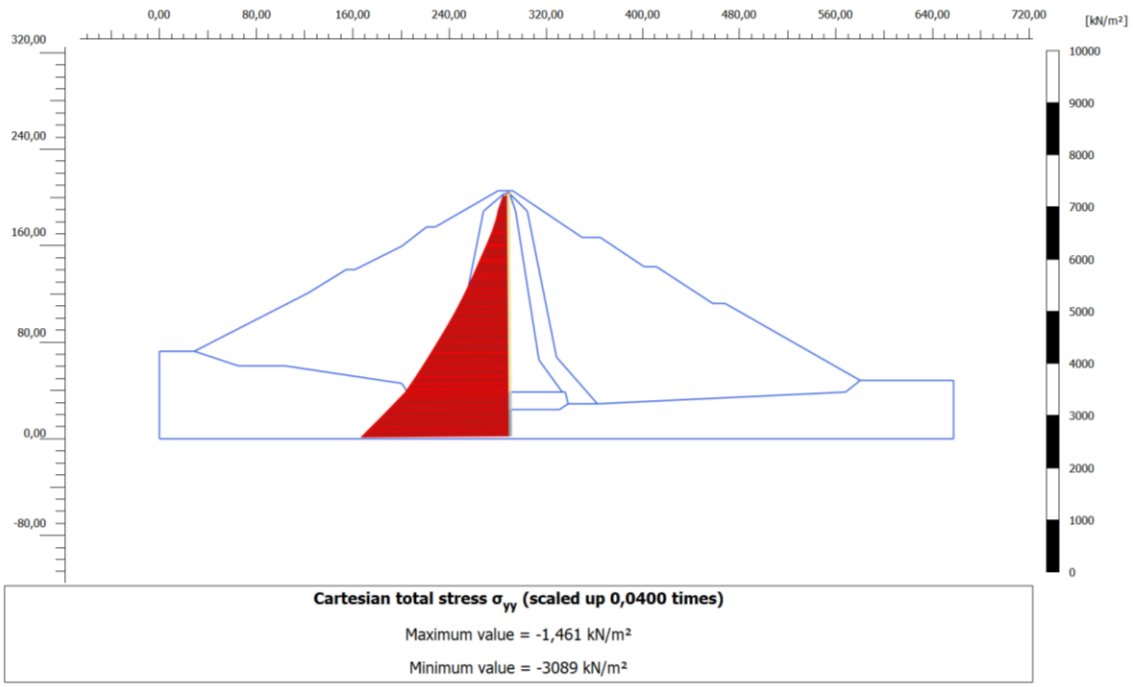

FIGURE 9. Vertical stress diagram at the middle of an earth dam

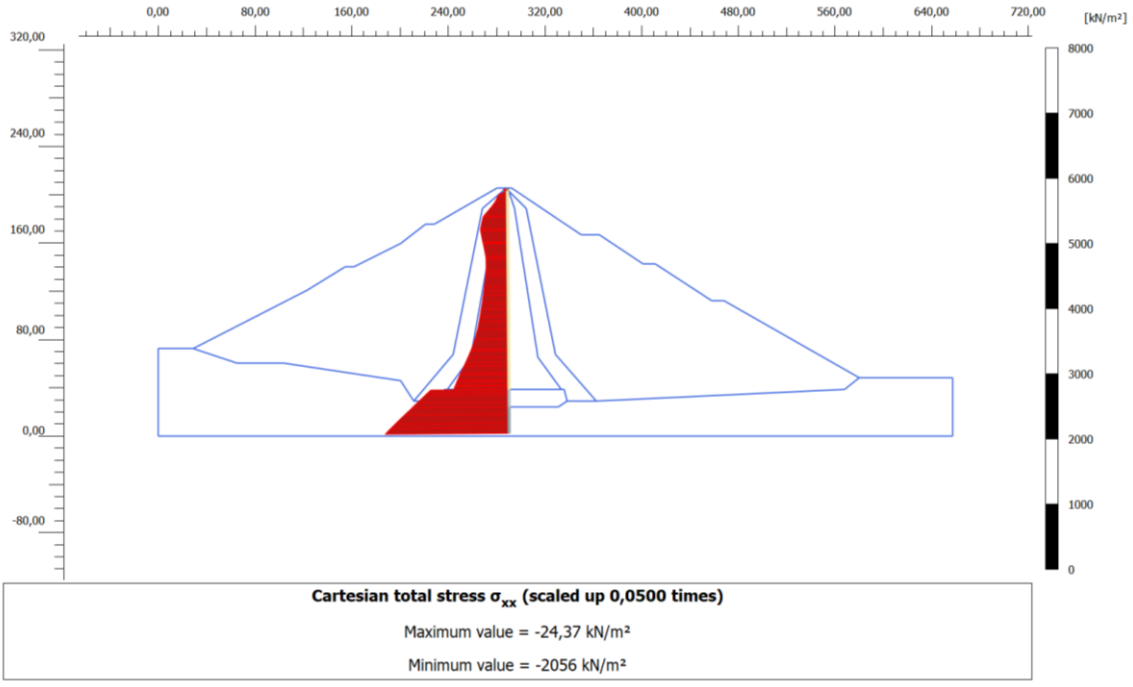

FIGURE 10. Horizontal stress diagram at the middle of an earth dam

ANALYSIS OF RESULTS

Figure 3 shows the change in horizontal and vertical stresses over time in the cross-section of an earth dam under the action of seismic forces. In this figure, the blue, green, black, and red curves represent stress changes at points A,

B, C, and D, respectively. Analyzing these figures, we can conclude that the greatest horizontal and vertical stresses occur at the lowest point, point D, i.e., the highest horizontal stress is -2 MPa, and the highest vertical stress is -3.6 MPa.

The contour line illustrating horizontal displacements in the cross-section of the earth dam is presented in Figure 4. The maximum-recorded horizontal displacement was 10.2 mm. Figure 5 displays the horizontal displacement diagram for the center of the earth dam. This horizontal displacement shifts to the right due to the water pressure from the left. In the center of the earth dam, the displacement increases from the bottom to the top, starting at zero at the bottom and reaching its maximum value at the very top. Figure 6 depicts the contour line of vertical displacements in the cross-section of the earth dam. The greatest vertical displacement of the earth dam is observed at the crest of the upper section, measuring -40.1 mm. Figure 7 illustrates the vertical displacements in the middle of the earth dam, indicating that the settlement at the base is zero, while the maximum displacement occurs in the upper section. Figure 8 presents the contour lines of vertical stresses in the cross-section of the earth dam. This figure shows that the highest vertical stress is located in the central lower part of the dam. Notably, the stress values on the slope above the water level and the right slope are zero. In Figure 9, the diagram of vertical stresses in the middle of the earth dam indicates that the maximum vertical stress is also zero, and the lower part exhibits a significant stress value of -3.09 MPa. Figure 10 illustrates the diagram of horizontal stresses in the middle of the earth dam. Here, we can conclude that the maximum value of vertical stress is zero, and, at the very bottom, it has a high value of -2.05 MPa.

CONCLUSION

- The stress-strain state of the Charvak earth dam was evaluated under seismic loading, considering the moisture content of the dam material along with water pressure and the dam's weight.
- Changes in horizontal and vertical stresses at key points of the dam were analyzed in response to seismic action.
- The static problem of the earth dam was addressed, resulting in the creation of isolines and diagrams that represent displacement and stress components, taking into account the moisture content of the dam material and water pressure.
- Analysis of the generated graphs, which account for water pressure, indicates that the greatest vertical displacements occurred at the top of the dam, with vertical stresses reaching -40.1 mm and horizontal stresses measuring 10.2 mm.

ACKNOWLEDGMENTS

This investigation was made possible by the funding provided by the Uzbekistan Academy of Sciences. We extend our deepest gratitude to the Academy for its unwavering support and dedication to advancing scientific research.

REFERENCES

1. K. Sultanov and S. Umarkhonov, Numerical calculation of an earth dam under elastic-plastic strain of soil subject to seismic impacts, in *International Conference: Ensuring Seismic Safety and Seismic Stability of Buildings and Structures, Applied Problems of Mechanics-2024*, AIP Conf. Proc. 3260, edited by R. A. Abirov et al. (AIP Publishing, Melville, NY, 2025), pp. 030009, https://doi.org/10.1063/5.0265101.
2. K. Sultanov, S. Umarkhonov, and S. Normatov, Calculation of earth dam strain under seismic impacts, in *International Conference on Actual Problems of Applied Mechanics - APAM-2021*, AIP Conf. Proc. 2637 (AIP Publishing, Melville, NY, 2022), pp. 030008, https://doi.org/10.1063/5.0118430.
3. M. M. Mostafa and S. Zhenzhong, Seepage behaviour through earth dams with zones of different filling materials, Water SA **50(1)**, 37 (2024), https://doi.org/10.17159/wsa/2024.v50.i1.4055.
4. A. Lashgari and R. E. S. Moss, Displacement and damage analysis of earth dams during the 2023 Turkey earthquake sequence, Earthquake Spectra **40(2)**, 939-976 (2024), https://doi.org/10.1177/87552930231223749.
5. M. Rashidi, M. Heidari, and G. Azizyan, Numerical analysis and monitoring of an embankment dam during construction and first impounding case study: Siah Sang Dam, Sci. Iran. **25(2)**, 505-516 (2018), https://doi.org/10.24200/sci.2017.4181.
6. K. Wei, S. Chen, G. Li, and H. Han, Application of a generalised plasticity model in high earth core dam static and dynamic analysis, Eur. J. Environ. Civ. Eng. **24(7)**, 979-1012 (2020), https://doi.org/10.1080/19648189.2018.1437777.

7. J. G. Xu, F. M. Wang, Y. H. Zhong, B. Wang, X. L. Li, and N. Sun, Stress analysis of polymer diaphragm wall for earth-rock dams under static and dynamic loads, Yantu Gongcheng Xuebao 34, 1613 (2012), https://doi.org/10.26480/iceti.01.2017.29.32.
8. C. Qi, W. Lu, J. Wu, and X. Liu, Application of effective stress model to analysis of liquefaction and seismic performance of an earth dam in China, Math. Probl. Eng. 2015, 571389 (2015), https://doi.org/10.1155/2015/404712.
9. M. P. Sainov and O. V. Anisimov, Stress-strain state of seepage-control wall constructed for repairs of earth rock-fill dam, Mag. Civ. Eng. **68(08)**, 3-17 (2016), https://doi.org/10.5862/MCE.68.1.
10. M. M. Mirsaidov, T. Z. Sultanov, and A. Sadullaev, Determination of the stress-strain state of earth dams with account of elastic-plastic and moist properties of soil and large strains, Mag. Civ. Eng. **40**, 59-68 (2013), https://doi.org/10.5862/MCE.40.7.
11. X. Yang and S. Chi, Seismic stability of earth-rock dams using finite element limit analysis. Soil Dyn. Earthquake Eng. **64**, 1-10 (2014), https://doi.org/10.1016/j.soildyn.2014.04.007.
12. C. Liu, L. Zhang, B. Bai, J. Chen, and J. Wang, Nonlinear analysis of stress and strain for a clay core rock-fill dam with FEM. Procedia Eng. **31**, 497-501 (2012), https://doi.org/10.1016/j.proeng.2012.01.1058.
13. H. Alateya and A. Ahangar Asr, Numerical investigation into the stability of earth dam slopes considering the effects of cavities. Eng. Comput. **37(4)**, 1397-1421 (2020), https://doi.org/10.1108/EC-03-2019-0101.
14. B. Ebrahimian, Numerical analysis of nonlinear dynamic behavior of earth dams. Front. Archit. Civ. Eng. China **5**, 24-40 (2011), https://doi.org/10.1007/s11709-010-0082-6.
15. M. M. Zanjani, A. Soroush, and M. Khoshini, Two-dimensional numerical modeling of fault rupture propagation through earth dams under steady state seepage. Soil Dyn. Earthquake Eng. **88**, 60-71 (2016), https://doi.org/10.1016/j.soildyn.2016.05.012.